AIAA JOURNAL
Vol. 37, No. 11, November 1999

Analytical Solution for Rectangular Thick Laminated Plates Subjected to Arbitrary Boundary Conditions

Senthil S. Vel* and R. C. Batra†
Virginia Polytechnic Institute and State University, Blacksburg, Virginia 24061

Three-dimensional deformations of a multilayered, linear elastic, anisotropic rectangular plate subjected to arbitrary boundary conditions at its edges are analyzed by the generalized Eshelby–Stroh formalism. The rectangular laminate consists of anisotropic and homogeneous laminae of arbitrary thicknesses. Perfect bonding is assumed between the adjoining laminae in the sense that both surface tractions and displacements are assumed to be continuous across their interfaces. The analytical solution is in terms of infinite series, and the effect of truncating the series on the accuracy of the solution is scrutinized. The method is also applicable to rectangular laminated plates, with edges of each lamina subjected to different boundary conditions. Results are presented for thick plates with different sets of edge boundary conditions, e.g., two opposite edges simply supported and the other two subjected to eight different conditions or all four edges clamped.

I. Introduction

FIBER-REINFORCED laminated plates are extensively used in aerospace, automotive, and ship-building industries primarily because of their high strength-to-weight ratio, and their strength and stiffness can be tailored to meet design requirements. The accurate prediction of the response characteristics of such laminated structures is a challenging task because of their intrinsic anisotropy, heterogeneity, and low ratio of the transverse shear modulus to the in-plane Young's modulus.

Laminated plates are usually analyzed by use of equivalent single-layer theories based on either the classical laminated plate theory[1,2] (CLPT), which assumes the Kirchhoff–Love hypothesis, or its refinements, such as the first-order shear deformation theory[2,3] (FSDT) and higher-order theories,[2,4–6] which include the effect of transverse shear deformations. Accurate prediction of interlaminar stresses is very important since they usually cause delamination failure at the interfaces. A drawback of equivalent single-layer theories is that they allow for discontinuous interlaminar stresses. Layerwise theories[7–10] are considerably more accurate than the preceding theories. We refer the reader to Refs. 2, 11, and 12 for a historical perspective and for a review of various approximate theories.

The validity of approximate plate theories can be assessed by comparing their predictions with the analytical solutions of the three-dimensional equations of anisotropic elasticity. Pagano,[13,14] Pagano and Hatfield,[15] Srinivas et al.,[16] and Srinivas and Rao[17] obtained analytical solutions for orthotropic simply supported laminates. These benchmark solutions have been used to validate new or improved plate theories and finite-element formulations.[7–11,18–22] However, simply supported edge conditions are less frequently realized in practice, and they do not exhibit the well-known boundary-layer effects observed near clamped or free edges.

Here we present analytical solutions for the deformations of anisotropic rectangular thick plates subjected to arbitrary boundary conditions. Each lamina may be generally anisotropic with 21 elastic constants and subjected to boundary conditions different from those on the adjoining laminae. The three-dimensional equations of elasticity are solved by a generalization of the Eshelby–Stroh formalism. Thus the governing equations are exactly satisfied, and various constants in the general solution are determined from the boundary conditions at the edges and continuity conditions at the interfaces. This results in an infinite system of equations in infinitely many unknowns. The truncation of this set of equations inevitably introduces errors that can be minimized by increasing the number of terms in the series. Results for plate problems with different sets of edge boundary conditions are presented in tabular form to facilitate comparison with predictions from various plate theories.

Received 10 September 1998; revision received 18 March 1999; accepted for publication 9 April 1999.

*Graduate Student, Department of Engineering Science and Mechanics, MC 0219.
†Clifton C. Garvin Professor, Department of Engineering Science and Mechanics, MC 0219.

II. Formulation of the Problem

We use a rectangular Cartesian coordinate system, shown in Fig. 1, to describe the infinitesimal quasi-static deformations of an N-layer anisotropic elastic laminate occupying the region $\mathcal{R} = [0, L_1] \times [0, L_2] \times [0, L_3]$ in the unstressed reference configuration. The vertical positions of the bottom and the top surfaces as well as of the $N-1$ interfaces between the laminae are denoted by $L_3^{(1)} = 0, L_3^{(2)}, \ldots, L_3^{(n)}, \ldots, L_3^{(N)}, L_3^{(N+1)} = L_3$.

Equations governing the displacements $\boldsymbol{u} = \boldsymbol{x} - \boldsymbol{X}$ of a material point $\boldsymbol{X}$ are

$$\sigma_{ij,j} = 0 \qquad (i, j = 1, 2, 3) \tag{1}$$

$$\sigma_{ij} = C_{ijkl}\varepsilon_{kl} \tag{2}$$

$$\varepsilon_{kl} = \tfrac{1}{2}(u_{k,l} + u_{l,k}) \tag{3}$$

Here $\boldsymbol{x}$ is the present position of the material particle that occupied place $\boldsymbol{X}$ in the reference configuration, σ_{ij} are the components of the Cauchy stress tensor, ε_{kl} are the components of the infinitesimal strain tensor, C_{ijkl} are elastic constants, a comma followed by index j indicates partial differentiation with respect to x_j, and a repeated index implies summation over the range of the index. We interchangeably use the direct and the indicial notation. The strain energy density W is given by

$$W = \tfrac{1}{2}C_{ijkl}\varepsilon_{ij}\varepsilon_{kl} \tag{4}$$

The symmetry of the stress tensor, symmetry of the strain tensor, and the existence of the strain energy function imply the following symmetry conditions:

$$C_{ijkl} = C_{jikl} = C_{klij} \tag{5}$$

Material elasticities are assumed to yield a positive strain energy density for every nonrigid deformation of the body. That is, $C_{ijkl}\varepsilon_{ij}\varepsilon_{kl} > 0$ for every nonzero symmetric tensor ε_{kl}. The strain energy U of the laminated plate is given by

$$U = \int_{\mathcal{R}} W \, dv \tag{6}$$

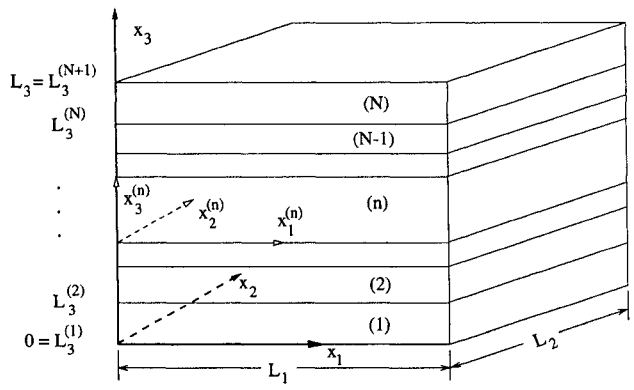

Fig. 1 An N-layer laminated rectangular plate.

The displacement or traction components on the side surfaces $x_1 = 0$, L_1 and $x_2 = 0$, L_2 and on the bottom and top surfaces $x_3 = 0$, L_3 are specified as

$$\boldsymbol{I}_u^{(s)}\boldsymbol{u} + \boldsymbol{I}_\sigma^{(s)}\boldsymbol{\sigma}_s = \boldsymbol{f}^{(s)} \quad \text{on} \quad x_s = 0$$

$$\boldsymbol{J}_u^{(s)}\boldsymbol{u} + \boldsymbol{J}_\sigma^{(s)}\boldsymbol{\sigma}_s = \boldsymbol{g}^{(s)} \quad \text{on} \quad x_s = L_s \qquad (s = 1, 2, 3) \quad (7)$$

(Ref. 23, pp. 497, 498), where $(\boldsymbol{\sigma}_s)_i = \sigma_{is}$. The functions $\boldsymbol{f}^{(s)}$ and $\boldsymbol{g}^{(s)}$ are known and $\boldsymbol{I}_u^{(s)}, \boldsymbol{I}_\sigma^{(s)}, \boldsymbol{J}_u^{(s)}$ and $\boldsymbol{J}_\sigma^{(s)}$ are 3×3 diagonal matrices. For most applications, these diagonal matrices have entries of either zero or one such that

$$\boldsymbol{I}_u^{(s)} + \boldsymbol{I}_\sigma^{(s)} = \boldsymbol{J}_u^{(s)} + \boldsymbol{J}_\sigma^{(s)} = \boldsymbol{I} \qquad (s = 1, 2, 3) \quad (8)$$

where $\boldsymbol{I}$ is the 3×3 identity matrix. For example, if the surface $x_1 = 0$ is rigidly clamped, then $\boldsymbol{I}_u^{(1)} = \boldsymbol{I}, \boldsymbol{I}_\sigma^{(1)} = \boldsymbol{0}$, and $\boldsymbol{f}^{(1)}(x_2, x_3) = \boldsymbol{0}$. Boundary conditions at a simply supported edge $x_1 = 0$ may be simulated by $\boldsymbol{I}_u^{(1)} = \text{diag}[0, 1, 1]$, $\boldsymbol{I}_\sigma^{(1)} = \text{diag}[1, 0, 0]$, and $\boldsymbol{f}^{(1)}(x_2, x_3) = \boldsymbol{0}$. The method is valid even when $\boldsymbol{I}_u^{(s)}, \boldsymbol{I}_\sigma^{(s)}, \boldsymbol{J}_u^{(s)}$, and $\boldsymbol{J}_\sigma^{(s)}$ are general matrices with elements functions of coordinates only. For a laminate on an elastic foundation, the diagonal matrices $\boldsymbol{I}_u^{(3)}, \boldsymbol{I}_\sigma^{(3)}, \boldsymbol{J}_u^{(3)}$, and $\boldsymbol{J}_\sigma^{(3)}$ may not satisfy Eq. (8). The interfaces between different laminae are assumed to be perfectly bonded together. Thus displacements and surface tractions between the adjoining laminae are taken to be continuous, that is,

$$[\![\boldsymbol{u}]\!] = \boldsymbol{0}, \qquad [\![\boldsymbol{\sigma}_3]\!] = \boldsymbol{0} \quad \text{on} \quad x_3 = L_3^{(2)}, L_3^{(3)}, \ldots, L_3^{(N)} \quad (9)$$

Here $[\![\boldsymbol{u}]\!]$ denotes the jump in the value of $\boldsymbol{u}$ across an interface.

III. Solution of the Governing Differential Equations

We construct a local coordinate system $x_1^{(n)}, x_2^{(n)}, x_3^{(n)}$ with local axes parallel to the global axes and the origin at the point where the global x_3 axis intersects the bottom surface of the nth lamina. In this local coordinate system, the nth lamina occupies the region $[0, l_1] \times [0, l_2] \times [0, l_3^{(n)}]$, where $l_1 = L_1, l_2 = L_2$, and $l_3^{(n)} = L_3^{(n+1)} - L_3^{(n)}$. We drop the superscript n for convenience with the understanding that all material constants and variables belong to this lamina.

The Eshelby–Stroh formalism[23–25] provides a solution for the generalized plane strain deformations of a linear elastic anisotropic material. Here we extend it to three-dimensional deformations by assuming that

$$\boldsymbol{u} = \boldsymbol{a}\exp\{i[(k_1\pi/l_1)x_1 + (k_2\pi/l_2)x_2 + p(x_3/l_3)]\} \quad (10)$$

where $\boldsymbol{a}$ and p are possible complex constants to be determined, k_1 and k_2 are known integers, and $i = \sqrt{-1}$. The chosen displacement field has a sinusoidal variation on the x_1–x_2 plane with an arbitrary exponential variation in the x_3 direction; k_1 and k_2 determine the period of the sinusoidal terms in the x_1 and the x_2 directions, respectively. From Eqs. (1–3) and (10), we obtain

$$\boldsymbol{D}(p)\boldsymbol{a} = \boldsymbol{0} \quad (11)$$

where

$$\boldsymbol{D}(p) = \boldsymbol{Q} + p(\boldsymbol{R} + \boldsymbol{R}^T) + p^2\boldsymbol{T}$$

$$Q_{jm} = \frac{k_1^2\pi^2}{l_1^2}C_{j1m1} + \frac{k_1k_2\pi^2}{l_1l_2}(C_{j1m2} + C_{j2m1}) + \frac{k_2^2\pi^2}{l_2^2}C_{j2m2}$$

$$R_{jm} = \frac{k_1\pi}{l_3l_1}C_{j3m1} + \frac{k_2\pi}{l_3l_2}C_{j3m2}, \qquad T_{jm} = \frac{1}{l_3^2}C_{j3m3} \quad (12)$$

Therefore p is a root of $\det[\boldsymbol{D}(p)] = 0$. For the strain energy density to be positive, the eigenvalues p cannot be real; it can be proved by following the arguments given by Ting (Ref. 23, pp. 135–136) for generalized plane strain deformations. Let $(p_\alpha, \boldsymbol{a}_\alpha)(\alpha = 1, 2, \ldots, 6)$ be eigensolutions of Eq. (11) such that

$$\text{Im}(p_\alpha) > 0, \qquad p_{\alpha+3} = \bar{p}_\alpha, \qquad \boldsymbol{a}_{\alpha+3} = \bar{\boldsymbol{a}}_\alpha \qquad (\alpha = 1, 2, 3) \quad (13)$$

where an overbar superimposed on a quantity denotes its complex conjugate. For distinct p_α we can superpose six solutions of the form of Eq. (10) to obtain

$$\boldsymbol{u} = \boldsymbol{A}\langle\exp\{i[(k_1\pi/l_1)x_1 + (k_2\pi/l_2)x_2 + p_*(x_3/l_3)]\}\rangle\boldsymbol{c} + \text{conjugate} \quad (14)$$

where $\boldsymbol{A} = [\boldsymbol{a}_1, \boldsymbol{a}_2, \boldsymbol{a}_3]$, $\boldsymbol{c}$ is an arbitrary 3×1 vector of unknown complex coefficients, $\langle\psi(p_*)\rangle = \text{diag}[\psi(p_1), \psi(p_2), \psi(p_3)]$, and conjugate stands for the complex conjugate of the explicitly stated term. The case of repeated eigenvalues is discussed in Sec. V. We obtain the following expressions for the stress tensor by substituting for $\boldsymbol{u}$ from Eq. (14) into Eq. (3) and the result into Eq. (2):

$$\boldsymbol{\sigma}_m = \boldsymbol{S}_m\langle\exp\{i[(k_1\pi/l_1)x_1 + (k_2\pi/l_2)x_2 + p_*(x_3/l_3)]\}\rangle\boldsymbol{c} + \text{conjugate} \quad (15)$$

where

$$\boldsymbol{S}_m = [\boldsymbol{E}_{(m,1)}\boldsymbol{a}_1, \boldsymbol{E}_{(m,2)}\boldsymbol{a}_2, \boldsymbol{E}_{(m,3)}\boldsymbol{a}_3]$$

$$[\boldsymbol{E}_{(\alpha,\beta)}]_{\gamma\delta} = i[(k_1\pi/l_1)C_{\gamma\alpha\delta1} + (k_2\pi/l_2)C_{\gamma\alpha\delta2} + (p_\beta/l_3)C_{\gamma\alpha\delta3}]$$

IV. Series Solution

The complete double Fourier series expansion constructed to satisfy the boundary/interface conditions on the surfaces $x_3^{(n)} = 0, l_3^{(n)}$ is obtained by superposing solutions of the form of Eq. (14). In the following equations the first superscript n denotes the nth lamina and the second superscript 3 indicates that the series terms have a double Fourier series expansion on the plane $x_3^{(n)} = \text{constant}$. The dependence of the eigenvalues and eigenvectors on k_1 and k_2 is indicated by the subscripts:

$$\begin{aligned}\boldsymbol{u}^{(n,3)}(x_1^{(n)}, x_2^{(n)}, x_3^{(n)}) &= \boldsymbol{A}_{(k_0,k_0)}^{(n,3)}[\boldsymbol{\eta}_{(k_0,k_0)}^{(n,3)}\boldsymbol{c}_{(k_0,k_0)}^{(n,3)} + \boldsymbol{\xi}_{(k_0,k_0)}^{(n,3)}\boldsymbol{d}_{(k_0,k_0)}^{(n,3)}] \\ &+ \sum_{k_1=1}^{\infty}\boldsymbol{A}_{(k_1,0)}^{(n,3)}[\boldsymbol{\eta}_{(k_1,0)}^{(n,3)}\boldsymbol{c}_{(k_1,0)}^{(n,3)} + \boldsymbol{\xi}_{(k_1,0)}^{(n,3)}\boldsymbol{d}_{(k_1,0)}^{(n,3)}] \\ &+ \sum_{k_2=1}^{\infty}\boldsymbol{A}_{(0,k_2)}^{(n,3)}[\boldsymbol{\eta}_{(0,k_2)}^{(n,3)}\boldsymbol{c}_{(0,k_2)}^{(n,3)} + \boldsymbol{\xi}_{(0,k_2)}^{(n,3)}\boldsymbol{d}_{(0,k_2)}^{(n,3)}] \\ &+ \sum_{k_1,k_2=1}^{\infty}\{\boldsymbol{A}_{(k_1,k_2)}^{(n,3)}[\boldsymbol{\eta}_{(k_1,k_2)}^{(n,3)}\boldsymbol{c}_{(k_1,k_2)}^{(n,3)} + \boldsymbol{\xi}_{(k_1,k_2)}^{(n,3)}\boldsymbol{d}_{(k_1,k_2)}^{(n,3)}] \\ &+ \boldsymbol{A}_{(k_1,-k_2)}^{(n,3)}[\boldsymbol{\eta}_{(k_1,-k_2)}^{(n,3)}\boldsymbol{c}_{(k_1,-k_2)}^{(n,3)} + \boldsymbol{\xi}_{(k_1,-k_2)}^{(n,3)}\boldsymbol{d}_{(k_1,-k_2)}^{(n,3)}]\} + \text{conjugate}\end{aligned} \quad (16)$$

The terms involving $k_0 \in (0, 1)$ play the role of the constant term in the double Fourier series expansion and

$$\eta^{(n,3)}_{(k_1,k_2)}(x_1^{(n)}, x_2^{(n)}, x_3^{(n)})$$

$$= \left\langle \exp\left\{ i\left[\frac{k_1\pi}{l_1}x_1^{(n)} + \frac{k_2\pi}{l_2}x_2^{(n)} + p^{(n,3)}_{(k_1,k_2,*)}\frac{x_3^{(n)}}{l_3^{(n)}} \right]\right\}\right\rangle$$

$$\xi^{(n,3)}_{(k_1,k_2)}(x_1^{(n)}, x_2^{(n)}, x_3^{(n)})$$

$$= \left\langle \exp\left(-i\left\{ \frac{k_1\pi}{l_1}x_1^{(n)} + \frac{k_2\pi}{l_2}x_2^{(n)} + p^{(n,3)}_{(k_1,k_2,*)}\left[\frac{x_3^{(n)}}{l_3^{(n)}} - 1 \right]\right\}\right)\right\rangle \tag{17}$$

The functions

$$\eta^{(n,3)}_{(k_1,k_2)}(x_1^{(n)}, x_2^{(n)}, x_3^{(n)}), \qquad \xi^{(n,3)}_{(k_1,k_2)}(x_1^{(n)}, x_2^{(n)}, x_3^{(n)})$$

vary sinusoidally on the surfaces $x_3^{(n)} = 0, l_3^{(n)}$ and exponentially in the $x_3^{(n)}$ direction. The first inequality in expressions (13) ensures that all functions decay exponentially toward the interior of the nth lamina.

Similar expressions can be written for $\boldsymbol{u}^{(n,1)}$ and $\boldsymbol{u}^{(n,2)}$, which have a complete double Fourier series expansion on the side surfaces $x_1^{(n)} = 0, l_1$ and $x_2^{(n)} = 0, l_2$, respectively. The displacement and stress fields for the nth lamina are

$$\boldsymbol{u}^{(n)}(x_1^{(n)}, x_2^{(n)}, x_3^{(n)}) = \sum_{s=1}^{3} \boldsymbol{u}^{(n,s)}[x_1^{(n)}, x_2^{(n)}, x_3^{(n)}]$$

$$\boldsymbol{\sigma}_m^{(n)}(x_1^{(n)}, x_2^{(n)}, x_3^{(n)}) = \sum_{s=1}^{3} \boldsymbol{\sigma}_m^{(n,s)}[x_1^{(n)}, x_2^{(n)}, x_3^{(n)}] \tag{18}$$

The unknowns $\boldsymbol{c}^{(n,s)}_{(k_1,k_2)}$ and $\boldsymbol{d}^{(n,s)}_{(k_1,k_2)}$ are assumed to be complex, except for $\boldsymbol{c}^{(n,s)}_{(k_0,k_0)}$ and $\boldsymbol{d}^{(n,s)}_{(k_0,k_0)}$, which are real.

V. Degeneracy of the Eigenvalues

The general solution given as Eq. (14) is applicable when the eigenvalues p_α are distinct. When one of the eigenvalues is a double root of $\det[\boldsymbol{D}(p)] = 0$, there may or may not be two corresponding independent eigenvectors $\boldsymbol{a}$ (Refs. 23 and 26). If there exist two independent eigenvectors associated with the double root, then the general solution can still be written as Eq. (14). When p is a double root with a single independent eigenvector, the first independent solution is given by Eq. (10) and a second independent solution is

$$\boldsymbol{u} = \frac{\mathrm{d}}{\mathrm{d}p}\left\{ \boldsymbol{a}\exp\left[i\left(\frac{k_1\pi}{l_1}x_1 + \frac{k_2\pi}{l_2}x_2 + p\frac{x_3}{l_3} \right)\right]\right\}$$

$$= \left(\frac{\mathrm{d}\boldsymbol{a}}{\mathrm{d}p} + i\frac{x_3}{l_3}\boldsymbol{a} \right)\exp\left[i\left(\frac{k_1\pi}{l_1}x_1 + \frac{k_2\pi}{l_2}x_2 + p\frac{x_3}{l_3} \right)\right] \tag{19}$$

where $\mathrm{d}\boldsymbol{a}/\mathrm{d}p$ is obtained by differentiating Eq. (11):

$$\boldsymbol{D}\frac{\mathrm{d}\boldsymbol{a}}{\mathrm{d}p} + \frac{\mathrm{d}\boldsymbol{D}}{\mathrm{d}p}\boldsymbol{a} = 0 \tag{20}$$

Dempsey and Sinclair[27] have shown the existence of a nontrivial solution to Eqs. (11) and (20) for $\boldsymbol{a}$ and $\mathrm{d}\boldsymbol{a}/\mathrm{d}p$. If p_1 is the double root and p_3 the single root, the general solution can be written as

$$\boldsymbol{u} = \boldsymbol{A}(x_3)\left\langle \exp\left[i\left(\frac{k_1\pi}{l_1}x_1 + \frac{k_2\pi}{l_2}x_2 + p_*\frac{x_3}{l_3} \right)\right]\right\rangle \boldsymbol{c} + \text{conjugate}$$

$$\boldsymbol{A}(x_3) = \left[\boldsymbol{a}_1, \left(\frac{\mathrm{d}\boldsymbol{a}_1}{\mathrm{d}p_1} + i\frac{x_3}{l_3}\boldsymbol{a}_1 \right), \boldsymbol{a}_3 \right] \tag{21}$$

where p_2 is set equal to p_1. The degenerate case of triple roots can be similarly analyzed.

VI. Satisfaction of Boundary and Interface Conditions

Boundary conditions (7) on the surfaces $x_s = 0, L_s$ and continuity conditions (9) on the interfaces $x_3 = L_3^{(2)}, L_3^{(3)}, \ldots, L_3^{(N)}$ are satisfied by the classical Fourier series method, resulting in a system of linear algebraic equations for the unknown coefficients $\boldsymbol{c}^{(n,s)}_{(k_1,k_2)}$ and $\boldsymbol{d}^{(n,s)}_{(k_1,k_2)}$.

On the bottom surface $x_3^{(1)} = 0$, we extend the component functions in Eqs. (18) defined on $[0, l_1] \times [0, l_2]$ to the interval $[-l_1, l_1] \times [-l_2, l_2]$. The functions $\eta^{(1,3)}_{(k_1,k_2)}$ and $\xi^{(1,3)}_{(k_1,k_2)}$, which have a sinusoidal variation on the plane $x_3^{(1)} = 0$, are extended without modification because they form the basis functions for this surface, except for terms involving k_0, which are extended as even functions. The functions $\eta^{(1,1)}_{(k_1,k_2)}$ and $\xi^{(1,1)}_{(k_1,k_2)}$, which have an exponential variation in the $x_1^{(1)}$ direction and a sinusoidal variation in the $x_2^{(1)}$ direction, are extended as even functions in the $x_1^{(1)}$ direction and without modification in the $x_2^{(1)}$ direction. The functions $\eta^{(1,2)}_{(k_1,k_2)}$ and $\xi^{(1,2)}_{(k_1,k_2)}$ are extended as even functions in the $x_2^{(1)}$ direction and without modification in the $x_1^{(1)}$ direction. The prescribed function $\boldsymbol{f}^{(3)}(x_1^{(1)}, x_2^{(1)})$ is suitably extended. We multiply the first equation of boundary conditions (7) that corresponds to $s = 3$ by

$$\exp\{i[\tilde{k}_1\pi x_1^{(1)}/l_1 + \tilde{k}_2\pi x_2^{(1)}/l_2]\}$$

and integrate the result with respect to $x_1^{(1)}$ and $x_2^{(1)}$ over the interval $[-l_1, l_1] \times [-l_2, l_2]$ to obtain

$$\int_{-l_2}^{l_2}\int_{-l_1}^{l_1} [\boldsymbol{I}_u^{(3)}\boldsymbol{u}^{(1)} + \boldsymbol{I}_\sigma^{(3)}\boldsymbol{\sigma}_3^{(1)} - \boldsymbol{f}^{(3)}]\exp\left\{ i\left[\frac{\tilde{k}_1\pi x_1^{(1)}}{l_1} + \frac{\tilde{k}_2\pi x_2^{(1)}}{l_2} \right]\right\}$$

$$\times \mathrm{d}x_1^{(1)}\,\mathrm{d}x_2^{(1)} = \boldsymbol{0} \quad \text{at} \quad x_3^{(1)} = 0 \tag{22}$$

for all $(\tilde{k}_1, \tilde{k}_2) \in (\{0\}, \{0\}) \cup (\mathcal{Z}^+ \times \{0\}) \cup (\{0\} \times \mathcal{Z}^+) \cup (\mathcal{Z}^+ \times \mathcal{Z}^+) \cup (\mathcal{Z}^+ \times \mathcal{Z}^-)$, where $\mathcal{Z}^+$ and $\mathcal{Z}^-$ denote the sets of positive and negative integers, respectively. The same procedure is repeated for the second equation of boundary conditions (7) on the top surface of the Nth lamina with $s = 3$ and interface continuity conditions (9) between the nth and the $(n+1)$th laminae.

On the side surfaces $x_1^{(n)} = 0, l_1$ the functions are extended over the interval $[-l_2, l_2] \times [-l_3^{(n)}, l_3^{(n)}]$ in the $x_2^{(n)} - x_3^{(n)}$ plane. We then multiply the second equation of boundary conditions (7) that corresponds to $s = 1$ by

$$\exp\{i[\tilde{k}_2\pi x_2^{(n)}/l_2 + \tilde{k}_3\pi x_3^{(n)}/l_3^{(n)}]\}$$

and integrate the result with respect to $x_2^{(n)}$ and $x_3^{(n)}$ over $[-l_2, l_2] \times [-l_3^{(n)}, l_3^{(n)}]$. A similar procedure is used to satisfy boundary condition (7) corresponding to $s = 2$ on the surfaces $x_2^{(n)} = 0, l_2$.

Substitution for $\boldsymbol{u}^{(n)}$ and $\boldsymbol{\sigma}_m^{(n)}$ from Eqs. (18) into Eq. (22) and the other equations that enforce the boundary conditions on the top surface, the lamina interfaces, and the side surfaces leads to an infinite set of linear algebraic equations for the infinitely many unknown coefficients $\boldsymbol{c}^{(n,s)}_{(k_1,k_2)}$ and $\boldsymbol{d}^{(n,s)}_{(k_1,k_2)}$. A general theory for the solution of the resulting infinite system of equations does not exist. However, reasonably accurate results can be obtained by truncating k_1 and k_2 in Eq. (16) to K_1 and K_2 terms, respectively. The series involving summations over k_2 and k_3 in the expression for $\boldsymbol{u}^{(n,1)}$ are truncated to K_2 and $K_3^{(n)}$ whereas those for $\boldsymbol{u}^{(n,2)}$ are truncated to $K_3^{(n)}$ and K_1 terms. In general, we try to maintain approximately the same period of the largest harmonic on all interfaces and boundaries by choosing $K_3^{(n)} = \mathrm{ceil}[K_1 l_3^{(n)}/l_1]$ and $K_2 = \mathrm{ceil}(K_1 l_2/l_1)$, where $\mathrm{ceil}(y)$ equals the smallest integer greater than or equal to y. Thus the size of the truncated matrix will depend solely on the choice of K_1.

VII. Results and Discussion

We present results for specific laminated plates. Each lamina is composed of a unidirectional fiber-reinforced material that is modeled as orthotropic and assigned the following stiffness properties[14]:

$$E_L/E_T = 25, \qquad G_{LT}/E_T = 0.5$$

$$G_{TT}/E_T = 0.2, \qquad \nu_{LT} = \nu_{TT} = 0.25 \tag{23}$$

where E, G, and ν denote Young's modulus, shear modulus, and Poisson's ratio, respectively, and subscripts L and T indicate directions parallel and perpendicular to the fibers, respectively. For values given in Eqs. (23), the nonzero components of the elastic tensor C_{ijkl} for a 0-deg lamina are

$$[C_{1111}, C_{2222}, C_{3333}] = [25.168, 1.071, 1.071]E_T$$

$$[C_{1122}, C_{1133}, C_{2233}] = [0.336, 0.336, 0.271]E_T$$

$$[C_{2323}, C_{3131}, C_{1212}] = [0.2, 0.5, 0.5]E_T \tag{24}$$

Such properties are typical of a high modulus graphite–epoxy composite.

The following three lamination schemes are considered:

1) A two-ply laminate with the fibers parallel to the x_1 and the x_2 directions in the bottom and the top layers, respectively, i.e., [0/90 deg] laminate

2) A three-ply laminate with the fibers parallel to the x_1, x_2, and x_1 directions in the bottom, middle, and top layers, respectively, i.e., [0/90/0 deg] laminate

3) A three-ply laminate with the fibers oriented at 45, −45, and 45 deg with respect to the x_1 axis on the x_1–x_2 plane in the bottom, middle, and top layers respectively, i.e., [45/−45/45 deg] laminate

The laminae are of equal thicknesses in all of the above cases. The following two load distributions are considered:

a) The top surface is subjected to a sinusoidal normal load, whereas the bottom surface is traction free:

$$\boldsymbol{f}^{(3)}(x_1, x_2) = \boldsymbol{0}$$

$$\boldsymbol{g}^{(3)}(x_1, x_2) = q_0[0, 0, \sin(\pi x_1/L_1)\sin(\pi x_2/L_2)]^T \tag{25}$$

i.e., $\sigma_{33}(x_1, x_2, H) = q_0 \sin(\pi x_1/L_1)\sin(\pi x_2/L_2)$. In this section we denote the thickness of the laminate by $H(=L_3)$.

b) The top surface is traction free, whereas the bottom surface is subjected to a sinusoidal normal load

$$\boldsymbol{f}^{(3)}(x_1, x_2) = -q_0[0, 0, \sin(\pi x_1/L_1)\sin(\pi x_2/L_2)]^T$$

$$\boldsymbol{g}^{(3)}(x_1, x_2) = \boldsymbol{0} \tag{26}$$

i.e., $\sigma_{33}(x_1, x_2, 0) = -q_0 \sin(\pi x_1/L_1)\sin(\pi x_2/L_2)$.

The displacements and stresses at specific locations on the x_1–x_2 plane and the strain energy are normalized as follows:

$$[\bar{u}_1(x_3), \bar{u}_2(x_3)] = \frac{100E_T H^2}{q_0 L_1^3}\left[u_1\left(\frac{L_1}{4}, \frac{L_2}{2}, x_3\right), u_2\left(\frac{L_1}{2}, \frac{L_2}{4}, x_3\right)\right]$$

$$\bar{u}_3(x_3) = \frac{100E_T H^3}{q_0 L_1^4} u_3\left(\frac{L_1}{2}, \frac{L_2}{2}, x_3\right)$$

$$\bar{e} = \frac{10E_T}{q_0 H}\left[u_3\left(\frac{L_1}{2}, \frac{L_2}{2}, H\right) - u_3\left(\frac{L_1}{2}\frac{L_2}{2}, 0\right)\right]$$

$$[\bar{\sigma}_{11}(x_3), \bar{\sigma}_{22}(x_3), \bar{\sigma}_{12}(x_3)] = \frac{10H^2}{q_0 L_1^2} \times \left[\sigma_{11}\left(\frac{L_1}{2}, \frac{L_2}{2}, x_3\right), \sigma_{22}\left(\frac{L_1}{2}, \frac{L_2}{2}, x_3\right), \sigma_{12}\left(\frac{L_1}{8}, 0, x_3\right)\right]$$

$$[\bar{\sigma}_{23}(x_3), \bar{\sigma}_{31}(x_3)] = \frac{10H}{q_0 L_1}\left[\sigma_{23}\left(\frac{L_1}{2}, 0, x_3\right), \sigma_{31}\left(\frac{L_1}{8}, \frac{L_2}{2}, x_3\right)\right]$$

$$\bar{\sigma}_{33}(x_3) = \frac{1}{q_0}\sigma_{33}\left(\frac{L_1}{2}, \frac{L_2}{2}, x_3\right), \qquad \bar{U} = \frac{E_T U}{q_0^2 L_1^3}$$

where $\bar{e}$ is the normalized elongation of the normal at the center of the plate. Note that the transverse normal, transverse shear, and in-plane stresses have been normalized differently so that the magnitude of each stress component is of the order of 1.

Table 1 Nomenclature for boundary conditions (BC) prescribed at $x_1 = 0$ or L_1

Notation	BC at $x_1 = 0$ or L_1	Corresponding $I_u^{(1)}$ or $J_u^{(1)}$	Name
B_1	$u_1 = 0, u_2 = 0, u_3 = 0$	diag[1, 1, 1]	Clamped surface
B_2	$u_1 = 0, u_2 = 0, \sigma_{13} = 0$	diag[1, 1, 0]	——
B_3	$u_1 = 0, \sigma_{12} = 0, u_3 = 0$	diag[1, 0, 1]	——
B_4	$u_1 = 0, \sigma_{12} = 0, \sigma_{13} = 0$	diag[1, 0, 0]	Slippery surface
B_5	$\sigma_{11} = 0, u_2 = 0, u_3 = 0$	diag[0, 1, 1]	Simply supported
B_6	$\sigma_{11} = 0, u_2 = 0, \sigma_{13} = 0$	diag[0, 1, 0]	——
B_7	$\sigma_{11} = 0, \sigma_{12} = 0, u_3 = 0$	diag[0, 0, 1]	——
B_8	$\sigma_{11} = 0, \sigma_{12} = 0, \sigma_{13} = 0$	diag[0, 0, 0]	Traction-free surface

A. Laminates with Two Opposite Edges Simply Supported

Here we consider laminates that are simply supported on the edges $x_2 = 0$, L_2 and subjected to eight different boundary conditions on the edges $x_1 = 0$ and L_1. In all cases $\boldsymbol{f}^{(1)} = \boldsymbol{g}^{(1)} = \boldsymbol{0}$, and $\boldsymbol{I}_u^{(s)}$, $\boldsymbol{I}_\sigma^{(s)}$, $\boldsymbol{J}_u^{(s)}$, and $\boldsymbol{J}_\sigma^{(s)}$ are diagonal matrices with entries 0 or 1 and satisfy Eq. (8). The nomenclature and definitions for the eight different boundary conditions are listed in Table 1. For example, when the surface $x_1 = 0$ is clamped and the surface $x_1 = L_1$ is traction free, we denote the configuration as B_1B_8. The present method can also analyze laminated plates when the edges of each lamina are subjected to boundary conditions different from those on the corresponding edges of the adjoining laminae. Such boundary conditions on the surface $x_1 = 0$ or L_1 are specified in the form $B_{(b_1,b_2,\ldots,b_N)}$, where the edge $x_1 = 0$ or L_1 of the nth lamina is subjected to boundary conditions B_{b_n}. This allows one to model realistically problems with varying boundary conditions on the edges.[28] For example, if the bottom lamina of a two-ply laminated plate is clamped at $x_1 = 0$ and L_1 and the corresponding edges of the top lamina are traction free, the configuration is denoted by $B_{(1,8)}B_{(1,8)}$.

When the laminae are orthotropic and the edges $x_2 = 0$, L_2 are simply supported, i.e., $u_1 = u_3 = 0$, $\sigma_{22} = 0$, a solution of the form

$$\boldsymbol{u} = [\hat{u}_1(x_1, x_3)\sin(\lambda\pi x_2/L_2), \hat{u}_2(x_1, x_3) \times \cos(\lambda\pi x_2/L_2), \hat{u}_3(x_1, x_3)\sin(\lambda\pi x_2/L_2)]^T \tag{27}$$

will satisfy boundary conditions at the simply supported edges. Thus we need only one term, namely, $k_2 = \lambda$, in the x_2 coordinate direction in the double Fourier series expansion, and the size of the truncated matrix can be greatly reduced.

Because any load distribution can be represented by a Fourier sine and cosine series and the problem being studied is linear, results for a general loading can be obtained by the method of superposition.

The effect of truncation of series on the solution is investigated for a square [0/90 deg] laminate that is simply supported on two opposite edges and clamped on the other two. Computed values of various variables at specific points in the laminate as well as the total strain energy are listed in Table 2. These results show that the normalized variables have converged to three decimal places with $K_1 = 250$ terms, while reasonable accuracy may be obtained with $K_1 = 25$ terms. Values of $\bar{\sigma}_{11}(0)$ computed with $K_1 = 150$, 200, and 250 slightly differ in the third decimal place but can be regarded as converged for all practical purposes. The upper and the lower values of the transverse normal and shear stresses are at corresponding points on the two sides of the interface between the two laminae. As is evident, the interface continuity conditions are also satisfied very well with increasing K_1. Positive values of $\bar{e}$ signify that the thickness of the plate at its centroid increases for the problem studied herein. The strain energy exhibits monotonic convergence from above and has converged to three decimal places for $K_1 = 50$. Although k_0 in Eq. (16) was chosen to be 0.5 for this study, a similar convergence behavior was observed for other values of k_0.

The normalized displacements and stresses for a square [0/90 deg] laminated plate with the edges $x_1 = 0$, L_1 subjected to various boundary conditions are given in Tables 3 and 4 for two different span-to-thickness ratios. Results in the last column of these tables are for the case in which the edges $x_1 = 0$ and L_1 of the bottom lamina are clamped and the corresponding edges of the upper

Table 2 Convergence study for a square [0/90 deg] laminate that is simply supported on two opposite edges and clamped on the other two: load (a), $L_1/H = 5$

K_1	$\bar{u}_1(H)$	$\bar{u}_3(\frac{1}{2}H^{\pm})$	$\bar{\sigma}_{11}(0)$	$\bar{\sigma}_{22}(H)$	$\bar{\sigma}_{33}(\frac{1}{2}H^{\pm})$	$\bar{\sigma}_{12}(0)$	$\bar{\sigma}_{23}(\frac{1}{2}H^{\pm})$	$\bar{\sigma}_{31}(\frac{1}{2}H^{\pm})$	$\bar{e}$	$\bar{U}$
25	−1.048053	1.221246	−4.638385	5.743101	0.574142	0.314157	0.876612	1.536511	5.280240	0.192923
		1.221196			0.581817		0.877367	1.538481		
50	−1.046988	1.218895	−4.625242	5.729313	0.579735	0.313719	0.875763	1.554877	5.265292	0.192409
		1.218900			0.577112		0.875531	1.554473		
100	−1.046800	1.217876	−4.632501	5.725563	0.578550	0.313323	0.875095	1.557369	5.268635	0.192176
		1.217875			0.579160		0.875158	1.557499		
150	−1.046807	1.217594	−4.629264	5.723659	0.578930	0.313253	0.874994	1.552760	5.267180	0.192114
		1.217594			0.578480		0.874964	1.552803		
200	−1.046821	1.217518	−4.631501	5.723726	0.578720	0.313240	0.874933	1.551250	5.267817	0.192095
		1.217518			0.578940		0.874950	1.551252		
250	−1.046817	1.217471	−4.629980	5.723184	0.578848	0.313234	0.874922	1.550322	5.267374	0.192084
		1.217471			0.578644		0.874910	1.550295		

Table 3 Displacements and stresses for a square [0/90 deg] laminate subjected to different BC: $L_1/H = 5$, $K_1 = 250$ terms

Theory	Variable	B_1B_1	B_2B_2	B_3B_3	B_4B_4	B_5B_5	B_6B_6	B_7B_7	B_8B_8	$B_{(1,8)}B_{(1,8)}$
Analytical, load (a)	$\bar{u}_1(H)$	−1.047	−0.512	−1.050	−0.343	−1.870	−0.847	−1.924	−0.565	−1.360
	$\bar{u}_2(0)$	1.341	2.632	1.360	3.247	1.899	2.717	1.961	3.291	1.490
	$\bar{u}_3(H/2)$	1.217	2.246	1.229	2.708	1.712	2.327	1.758	2.753	1.343
	$\bar{\sigma}_{11}(0)$	−4.630	−2.499	−4.667	−1.994	−7.671	−3.457	−7.913	−2.660	−4.872
	$\bar{\sigma}_{22}(H)$	5.723	10.568	5.771	12.705	7.894	10.888	8.096	12.877	6.263
	$\bar{\sigma}_{33}(H/2)$	0.579	0.432	0.577	0.368	0.495	0.416	0.489	0.359	0.576
	$\bar{\sigma}_{12}(0)$	0.313	0.487	0.247	0.065	0.527	0.539	0.424	0.108	0.353
	$\bar{\sigma}_{23}(H/2)$	0.875	1.351	0.871	1.499	1.211	1.416	1.225	1.541	0.949
	$\bar{\sigma}_{31}(H/2)$	1.550	0.638	1.567	0.419	1.216	0.638	1.195	0.416	0.909
	$\bar{e}$	5.267	6.057	5.280	6.438	4.733	5.748	4.734	6.233	5.164
Analytical, load (b)	$\bar{u}_1(H)$	−1.043	−0.512	−1.046	−0.345	−1.899	−0.892	−1.953	−0.619	−1.366
	$\bar{u}_2(0)$	1.295	2.578	1.312	3.182	1.870	2.676	1.931	3.238	1.446
	$\bar{u}_3(H/2)$	1.203	2.226	1.214	2.681	1.712	2.318	1.757	2.735	1.331
	$\bar{\sigma}_{11}(0)$	−4.871	−2.751	−4.905	−2.254	−7.894	−3.743	−8.128	−2.965	−5.122
	$\bar{\sigma}_{22}(H)$	5.441	10.259	5.486	12.360	7.671	10.618	7.870	12.567	5.990
	$\bar{\sigma}_{33}(H/2)$	−0.409	−0.555	−0.410	−0.618	−0.495	−0.573	−0.501	−0.629	−0.412
	$\bar{\sigma}_{12}(0)$	0.305	0.478	0.244	0.063	0.523	0.535	0.424	0.114	0.345
	$\bar{\sigma}_{23}(H/2)$	0.974	1.447	0.971	1.594	1.316	1.517	1.330	1.640	1.050
	$\bar{\sigma}_{31}(H/2)$	1.452	0.547	1.467	0.330	1.119	0.547	1.095	0.326	0.79
	$\bar{e}$	−4.153	−3.367	−4.141	−2.993	−4.733	−3.733	−4.734	−3.261	−4.260
HSDT[29]	$\bar{u}_3(H/2)$	1.088	—	—	—	1.667	—	—	2.624	—
	$\bar{\sigma}_{11}(0)$	−5.679	—	—	—	−8.385	—	—	−3.171	—
	$\bar{\sigma}_{22}(H)$	5.505	—	—	—	8.385	—	—	13.551	—
	$\bar{\sigma}_{23}(H/2)$	2.095	—	—	—	3.155	—	—	4.457	—
FSDT[29]	$\bar{u}_3(H/2)$	1.257	—	—	—	1.758	—	—	2.777	—
	$\bar{\sigma}_{11}(0)$	−3.911	—	—	—	−7.157	—	—	−2.469	—
	$\bar{\sigma}_{22}(H)$	5.153	—	—	—	7.157	—	—	11.907	—
	$\bar{\sigma}_{23}(H/2)$	1.958	—	—	—	2.729	—	—	3.901	—
CLPT[29]	$\bar{u}_3(H/2)$	0.429	—	—	—	1.064	—	—	1.777	—
	$\bar{\sigma}_{11}(0)$	−4.800	—	—	—	−7.157	—	—	−2.403	—
	$\bar{\sigma}_{22}(H)$	2.914	—	—	—	7.157	—	—	11.849	—

lamina are traction free. The value of $\bar{\sigma}_{22}(H)$ for $L_1/H = 5$ decreases from 12.877 to 6.263 when the boundary conditions on the edges $x_1 = 0, L_1$ of the bottom lamina are changed from traction free to clamped; the effect on the other variables is also quite noticeable. A comparison of results for configurations B_1B_1 with those for $B_{(1,8)}B_{(1,8)}$ reveals that altering the boundary conditions on the edges $x_1 = 0, L_1$ of the upper lamina from clamped to traction free has a noticeable effect on the values of $\bar{u}_1(H)$ and $\bar{\sigma}_{31}(H/2)$. We compare our results with those of Khdeir and Reddy,[29] who analyzed the problem with the classical lamination theory, FSDT, and third-order shear deformation theory[6] (HSDT). They considered six different sets of boundary conditions on two opposite edges whereas the other two edges were simply supported. However, we compare results for configurations B_1B_1, B_5B_5, and B_8B_8. Our results indicate that the displacements and stresses at a point depend on whether the normal load is applied on the top or the bottom surface of the laminate, whereas laminated plate theories yield the same results irrespective of the surface on which the load is applied. The CLPT and the HSDT underestimate the deflection at the center of the plate whereas FSDT overestimates it. The results obtained from the equivalent single-layer theories are close to our analytical values for large span-to-thickness ratios, except for the transverse shear stress $\bar{\sigma}_{23}(H/2)$. The HSDT has errors of ~10 and 20% in predicting the displacement $u_3(H/2)$ and normal stress $\sigma_{11}(0)$, respectively, for configuration B_1B_1, with $L_1/H = 5$. These errors decrease to 5 and 6%, respectively, for a span-to-thickness ratio of $L_1/H = 10$. Our computed value of $\bar{\sigma}_{23}(H/2)$ for a square [0/90 deg] laminate with $L_1/H = 4$ matches very well with that of Lee and Cao[19] for plates that are simply supported on all edges, but differs from that given by Khdeir and Reddy.[29]

Figure 2 depicts the through-thickness distribution of the in-plane normal stress $\bar{\sigma}_{11}$ on four sections, $x_1/L_1 = 0.05, 0.1, 0.3$, and 0.5, for a square [0/90 deg] laminated plate of $L_1/H = 5$, simply supported on edges $x_2 = 0, L_2$ and clamped on $x_1 = 0, L_1$, and loaded by a sinusoidally distributed load on the top surface. Whereas in the upper lamina with fibers along the x_2 axis the distribution of σ_{11} on the four sections is qualitatively similar to each other with magnitude close to zero, that in the lower lamina with fibers along the x_1 axis is quite different. As expected, the lower lamina with higher stiffness in the x_1 direction provides more resistance to bending in the x_1–x_3 plane. Similarly, the upper lamina provides significant resistance to bending in the x_2–x_3 plane.

Table 4 Displacements and stresses for a square [0/90 deg] laminate subjected to different BC: $L_1/H = 10$, $K_1 = 250$ terms

Theory	Variable	B_1B_1	B_2B_2	B_3B_3	B_4B_4	B_5B_5	B_6B_6	B_7B_7	B_8B_8	$B_{(1,8)}B_{(1,8)}$
Analytical, load (a)	$\bar{u}_1(H)$	−0.976	−0.576	−0.977	−0.293	−1.776	−1.079	−1.806	−0.541	−1.102
	$\bar{u}_2(0)$	0.933	2.043	0.936	2.932	1.782	2.280	1.821	3.004	1.056
	$\bar{u}_3(H/2)$	0.649	1.387	0.651	1.975	1.227	1.550	1.254	2.026	0.732
	$\bar{\sigma}_{11}(0)$	−4.653	−2.941	−4.660	−1.838	−7.304	−4.427	−7.432	−2.503	−4.853
	$\bar{\sigma}_{22}(H)$	3.888	8.302	3.897	11.812	7.309	9.250	7.465	12.100	4.373
	$\bar{\sigma}_{33}(H/2)$	0.64	0.49	0.64	0.37	0.50	0.45	0.49	0.36	0.65
	$\bar{\sigma}_{12}(0)$	0.221	0.310	0.208	0.052	0.497	0.432	0.470	0.119	0.256
	$\bar{\sigma}_{23}(H/2)$	0.713	1.113	0.714	1.423	1.219	1.292	1.241	1.490	0.780
	$\bar{\sigma}_{31}(H/2)$	1.592	0.794	1.598	0.361	1.154	0.764	1.130	0.374	0.90
	$\bar{e}$	4.684	9.304	4.693	12.965	4.733	8.278	4.779	12.275	4.642
Analytical, load (b)	$\bar{u}_1(H)$	−0.977	−0.579	−0.977	−0.297	−1.782	−1.090	−1.812	−0.557	−1.104
	$\bar{u}_2(0)$	0.925	2.030	0.927	2.913	1.776	2.270	1.815	2.989	1.048
	$\bar{u}_3(H/2)$	0.648	1.382	0.649	1.967	1.227	1.547	1.254	2.020	0.731
	$\bar{\sigma}_{11}(0)$	−4.681	−2.977	−4.688	−1.880	−7.309	−4.455	−7.436	−2.545	−4.881
	$\bar{\sigma}_{22}(H)$	3.876	8.269	3.885	11.759	7.304	9.230	7.460	12.059	4.362
	$\bar{\sigma}_{33}(H/2)$	−0.36	−0.51	−0.36	−0.63	−0.50	−0.54	−0.51	−0.64	−0.35
	$\bar{\sigma}_{12}(0)$	0.219	0.308	0.207	0.051	0.495	0.430	0.469	0.121	0.254
	$\bar{\sigma}_{23}(H/2)$	0.743	1.142	0.744	1.450	1.249	1.322	1.271	1.519	0.810
	$\bar{\sigma}_{31}(H/2)$	1.562	0.768	1.567	0.337	1.126	0.738	1.101	0.350	0.87
	$\bar{e}$	−4.751	−0.152	−4.742	3.488	−4.733	−1.217	−4.688	2.749	−4.793
HSDT[29]	$\bar{u}_3(H/2)$	0.617	—	—	—	1.216	—	—	1.992	—
	$\bar{\sigma}_{11}(0)$	−4.952	—	—	—	−7.468	—	—	−2.624	—
	$\bar{\sigma}_{22}(H)$	3.803	—	—	—	7.468	—	—	12.295	—
	$\bar{\sigma}_{23}(H/2)$	1.725	—	—	—	3.190	—	—	4.489	—
FSDT[29]	$\bar{u}_3(H/2)$	0.656	—	—	—	1.237	—	—	2.028	—
	$\bar{\sigma}_{11}(0)$	−4.450	—	—	—	−7.157	—	—	−2.442	—
	$\bar{\sigma}_{22}(H)$	3.799	—	—	—	7.157	—	—	11.884	—
	$\bar{\sigma}_{23}(H/2)$	1.523	—	—	—	2.729	—	—	3.882	—
CLPT[29]	$\bar{u}_3(H/2)$	0.429	—	—	—	1.064	—	—	1.777	—
	$\bar{\sigma}_{11}(0)$	−4.800	—	—	—	−7.157	—	—	−2.403	—
	$\bar{\sigma}_{22}(H)$	2.914	—	—	—	7.157	—	—	11.849	—

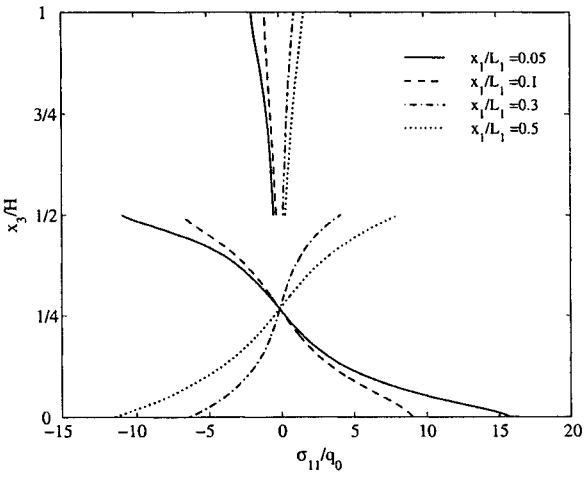

Fig. 2 Normal stress distribution on four sections of a square [0/90 deg] laminate that is simply supported on two opposite edges and clamped on the other two: load (a), $x_2 = L_2/2$, $L_1/H = 5$, $K_1 = 250$ terms.

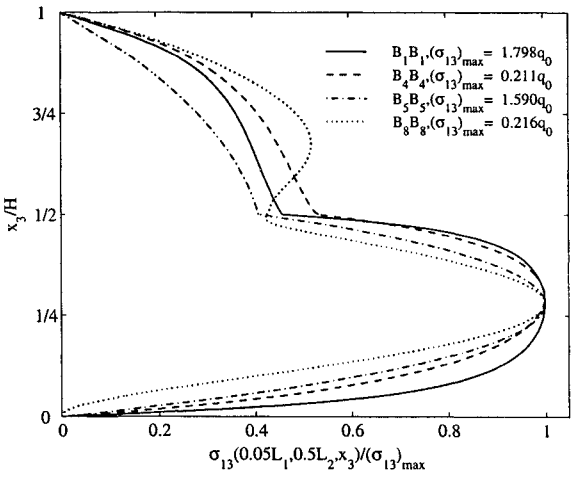

Fig. 3 Influence of the boundary conditions on the through-thickness distribution of the transverse shear stress σ_{13} for a square [0/90 deg] laminate: load (a), $L_1/H = 5$, $K_1 = 250$ terms.

The through-thickness distribution of the transverse shear stresses near the edge $x_1 = 0$, plotted in Figs. 3 and 4, shows that the shape of the distribution depends on the boundary conditions applied at the edge. The transverse shear stresses are not parabolic, as is usually assumed, and in fact their slopes are discontinuous at the layer interfaces. The layerwise models of Ren[9] and Lee et al.[10] that assume a parabolic variation of the transverse shear stress provide a better approximation than Reddy's theory[6] that is based on the parabolic variation of the transverse shear strain. Good results should be obtained when the assumed transverse shear-stress distribution is close to the analytical one obtained here. As noted by Lee and Cao,[19] such a distribution is not known a priori because it depends on the lamination scheme, plate geometry, boundary conditions, and loading. Moreover, our results indicate that a single continuously differentiable function will not describe well the through-thickness distribution of the transverse shear stress at all points on the x_1–x_2 plane of the laminate.

The transverse normal stress vs x_1 at $x_2 = L_2/2$ is plotted in Fig. 5 for a square [0/90 deg] laminate that is subjected to the layerwise boundary conditions $B_{(1,8)}B_{(1,8)}$. It exhibits severe gradients at points on the interface that are close to the edges. This may be due to the presence of a stress singularity on the lines where the interface meets the edges $x_1 = 0$ and L_1. The change in the thickness of a square [0/90 deg] laminate that is simply supported on two opposite edges and traction free on the other two is shown in Fig. 6. The variation over only a quarter of the plate is shown because of the symmetry of the loading and the boundary conditions about the two centroidal axes. Although the change in thickness is zero at the simply supported edges, as expected, it is not negligible at the free edges. The change in thickness is maximum at the center of the plate.

Table 5 gives, for eight different boundary conditions, the normalized displacements and stresses in a square [0/90/0 deg] laminate with $L_1/H = 5$, 10. Because the laminate is symmetric about the

Table 5 Displacements and stresses for a square [0/90/0 deg] laminate subjected to eight different BC: load (a), $K_1 = 250$ terms

L_1/H	Variable	B_1B_1	B_2B_2	B_3B_3	B_4B_4	B_5B_5	B_6B_6	B_7B_7	B_8B_8
5	$\bar{u}_1(0)$	0.319	0.162	0.321	0.090	0.614	0.227	0.628	0.108
	$\bar{u}_1(H)$	−0.331	−0.175	−0.333	−0.103	−0.620	−0.233	−0.634	−0.114
	$\bar{u}_2(0)$	1.053	3.281	1.061	5.007	1.353	3.312	1.376	5.015
	$\bar{u}_2(H)$	−1.044	−3.272	−1.051	−4.998	−1.346	−3.304	−1.369	−5.007
	$\bar{u}_3(H/2)$	1.180	3.503	1.188	5.297	1.525	3.542	1.550	5.307
	$\bar{\sigma}_{11}(0)$	−4.235	−2.660	−4.253	−1.897	−6.987	−3.238	−7.121	−2.043
	$\bar{\sigma}_{11}(H)$	4.504	2.928	4.520	2.164	7.180	3.431	7.312	2.232
	$\bar{\sigma}_{22}(H/3)$[a]	−3.726	−11.332	−3.753	−17.221	−4.784	−11.442	−4.864	−17.247
	$\bar{\sigma}_{22}(2H/3)$[a]	3.573	11.179	3.599	17.067	4.639	11.297	4.718	17.102
	$\bar{\sigma}_{33}(H/2)$	0.495	0.495	0.495	0.495	0.496	0.496	0.496	0.496
	$\bar{\sigma}_{33}(2H/3)$	0.701	0.748	0.702	0.786	0.726	0.757	0.727	0.790
	$\bar{\sigma}_{12}(0)$	0.256	0.548	0.221	0.048	0.404	0.578	0.346	0.059
	$\bar{\sigma}_{12}(H)$	−0.257	−0.548	−0.223	−0.050	−0.403	−0.578	−0.349	−0.061
	$\bar{\sigma}_{23}(H/2)$	1.470	3.980	1.478	5.905	1.911	4.033	1.939	5.917
	$\bar{\sigma}_{31}(H/2)$	2.093	1.028	2.102	0.459	2.653	1.330	2.677	0.617
	$\bar{e}$	4.694	4.693	4.694	4.693	4.715	4.714	4.715	4.715
10	$\bar{u}_1(0)$	0.227	0.150	0.227	0.062	0.522	0.276	0.527	0.075
	$\bar{u}_1(H)$	−0.227	−0.151	−0.227	−0.062	−0.520	−0.274	−0.525	−0.072
	$\bar{u}_2(0)$	0.465	2.216	0.466	4.731	0.782	2.282	0.790	4.734
	$\bar{u}_2(H)$	−0.460	−2.211	−0.461	−4.725	−0.777	−2.277	−0.785	−4.729
	$\bar{u}_3(H/2)$	0.446	2.089	0.447	4.449	0.753	2.155	0.760	4.453
	$\bar{\sigma}_{11}(0)$	−3.000	−2.278	−3.002	−1.440	−5.898	−3.509	−5.952	−1.562
	$\bar{\sigma}_{11}(H)$	3.032	2.309	3.034	1.472	5.906	3.516	5.959	1.569
	$\bar{\sigma}_{22}(H/3)$[a]	−1.713	−8.068	−1.715	−17.194	−2.882	−8.314	−2.909	−17.205
	$\bar{\sigma}_{22}(2H/3)$[a]	1.674	8.029	1.676	17.155	2.845	8.277	2.871	17.168
	$\bar{\sigma}_{33}(H/2)$	0.50	0.50	0.50	0.50	0.50	0.50	0.50	0.50
	$\bar{\sigma}_{33}(2H/3)$	0.73	0.76	0.73	0.81	0.74	0.76	0.74	0.81
	$\bar{\sigma}_{12}(0)$	0.124	0.208	0.121	0.026	0.268	0.264	0.260	0.032
	$\bar{\sigma}_{12}(H)$	−0.123	−0.207	−0.121	−0.025	−0.266	−0.263	−0.259	−0.031
	$\bar{\sigma}_{23}(H/2)$	0.722	2.867	0.723	5.955	1.228	2.996	1.239	5.963
	$\bar{\sigma}_{31}(H/2)$	3.062	1.957	3.064	0.618	3.301	2.148	3.310	0.694
	$\bar{e}$	4.714	4.714	4.714	4.714	4.727	4.727	4.728	4.728

[a] Values corresponding to the central layer.

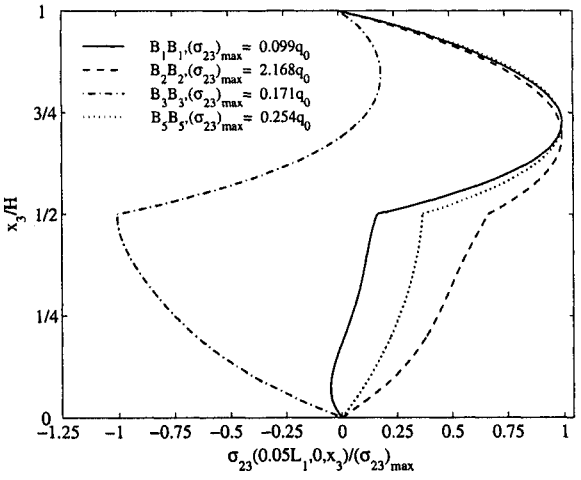

Fig. 4 Influence of the boundary conditions on the through-thickness distribution of the transverse shear stress σ_{23} for a square [0/90 deg] laminate: load (a), $L_1/H = 5$, $K_1 = 250$ terms.

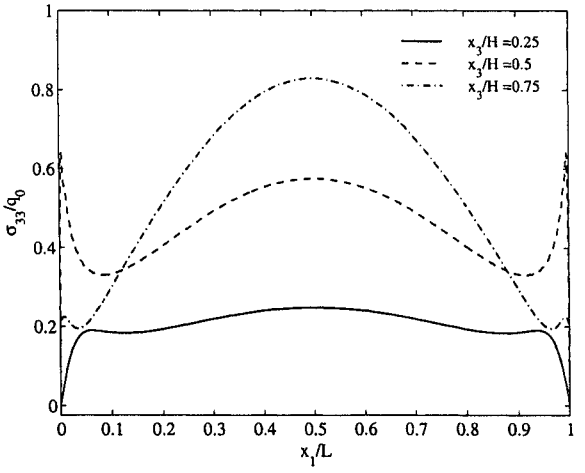

Fig. 5 Variation in the longitudinal direction of the transverse normal stress at $x_2 = L_2/2$ for a square [0/90 deg] laminate subjected to layerwise variation of the boundary conditions: configuration $B_{(1,8)}B_{(1,8)}$, load (a), $L_1/H = 5$, $K_1 = 250$ terms.

midplane, results are given only for normal loading on the top surface. The in-plane normal stress $\bar{\sigma}_{11}$ on the top surface of thick laminates is considerably larger in magnitude than those on the bottom surface. This asymmetry is attributed to the external loads being applied on the top surface whereas the bottom surface is traction free and is less for the thinner laminate. Different plate theories do not predict this asymmetry. We retrieve Pagano's results[14] when all four edges of the laminate are simply supported. The transverse displacement or the deflection of the centroid of the plate and the magnitude of $\bar{\sigma}_{11}(0)$ are considerably less when the edges $x_1 = 0, L_1$ are clamped, compared with those when the edges are simply supported. Recall that the other two edges are simply supported in each case. However, for the symmetric thick laminate, the change in the thickness of the plate at its centroid is essentially the same for each one of the eight sets of boundary conditions. The average elongation $\bar{e}$ at the center of the antisymmetric [0/90 deg] laminate is much more sensitive to the boundary conditions in the thin plate than in the thick plate (see Tables 3 and 4). For example, in Table 4 corresponding to load (b) we see that the normal at the center may elongate or contract depending on the boundary conditions at the edges of the plate. We can explain this by observing that the stresses σ_{11} and σ_{22} are of the order of $q_0L_1^2/H^2$ whereas the transverse normal stress σ_{33} is of the order of q_0. Thus the in-plane normal stresses dominate over the transverse normal stress for thin plates. For orthotropic materials the transverse normal strain $\varepsilon_{33} = -\nu_{13}\sigma_{11}/E_1 - \nu_{23}\sigma_{22}/E_2 + \sigma_{33}/E_3$, and for thin laminates Poisson's elongation/contraction that is due to σ_{11} and σ_{22} will exceed that which is due to σ_{33}. Since the normal stresses σ_{11} and σ_{22} at the center of the laminate are sensitive to the boundary conditions, the elongation of

Table 6 Through-thickness displacement and stress distributions for a square [0/90/0 deg] laminate that is simply supported on two opposite edges and clamped on the other two: load (a), $L_1/H = 5$, $K_1 = 250$ terms

x_3/H	$\bar{u}_1$	$\bar{u}_2$	$\bar{u}_3$	$\bar{\sigma}_{11}$	$\bar{\sigma}_{22}$	$\bar{\sigma}_{33}$	$\bar{\sigma}_{12}$	$\bar{\sigma}_{23}$	$\bar{\sigma}_{31}$
0.00	0.319	1.053	1.152	−4.235	−0.510	0.001	0.256	0.000	0.000
0.05	0.201	0.929	1.155	−2.811	−0.440	0.012	0.211	0.123	1.646
0.10	0.118	0.813	1.158	−1.732	−0.374	0.043	0.176	0.227	2.609
0.15	0.057	0.704	1.160	−0.894	−0.313	0.088	0.146	0.314	3.078
0.20	0.007	0.600	1.162	−0.198	−0.254	0.141	0.120	0.384	3.227
0.25	−0.039	0.500	1.165	0.448	−0.198	0.198	0.094	0.440	3.101
0.30	−0.091	0.403	1.167	1.121	−0.142	0.254	0.067	0.482	2.643
$(1/3)^-$	−0.132	0.339	1.169	1.617	−0.106	0.290	0.047	0.501	2.138
$(1/3)^+$	−0.132	0.339	1.169	0.057	−3.726	0.290	0.047	0.501	2.138
0.35	−0.117	0.302	1.170	0.055	−3.306	0.308	0.042	0.688	2.132
0.40	−0.073	0.198	1.173	0.051	−2.145	0.366	0.028	1.120	2.113
0.45	−0.030	0.103	1.176	0.047	−1.087	0.429	0.016	1.377	2.100
0.50	0.012	0.013	1.180	0.043	−0.080	0.495	0.004	1.470	2.093
0.55	0.053	−0.078	1.184	0.039	0.929	0.561	−0.007	1.404	2.093
0.60	0.094	−0.173	1.188	0.036	1.988	0.625	−0.020	1.174	2.100
0.65	0.134	−0.277	1.193	0.034	3.152	0.683	−0.034	0.767	2.111
$(2/3)^-$	0.147	−0.315	1.194	0.033	3.573	0.701	−0.040	0.589	2.114
$(2/3)^+$	0.147	−0.315	1.194	−1.692	0.193	0.701	−0.040	0.589	2.114
0.70	0.104	−0.376	1.198	−1.169	0.229	0.738	−0.060	0.561	2.668
0.75	0.049	−0.471	1.203	−0.458	0.284	0.795	−0.087	0.508	3.180
0.80	0.000	−0.572	1.208	0.225	0.342	0.854	−0.113	0.439	3.340
0.85	−0.053	−0.678	1.213	0.964	0.402	0.909	−0.140	0.356	3.208
0.90	−0.118	−0.791	1.218	1.852	0.466	0.956	−0.171	0.256	2.734
0.95	−0.206	−0.913	1.223	2.995	0.534	0.988	−0.208	0.138	1.732
1.00	−0.331	−1.044	1.227	4.504	0.609	0.999	−0.257	0.000	0.000

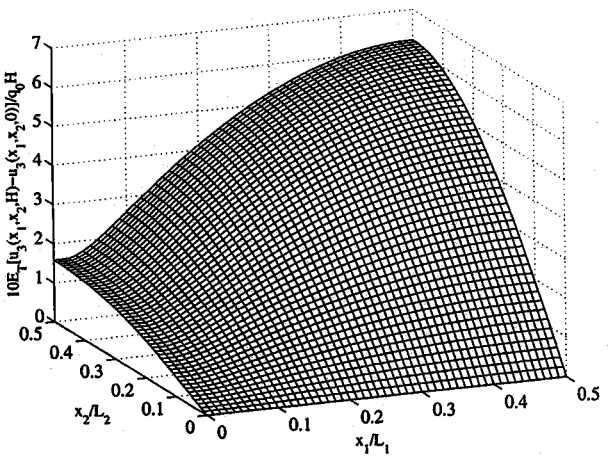

Fig. 6 Change in thickness of a square [0/90 deg] laminate that is simply supported on two edges and traction free on the other two: load (a), $L_1/H = 5$, $K_1 = 250$ terms.

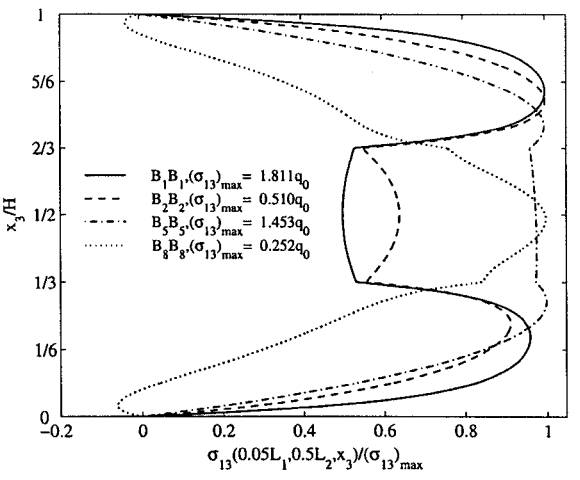

Fig. 7 Influence of the boundary conditions on the through-thickness distribution of the transverse shear stress σ_{13} for a square [0/90/0 deg] laminate: load (a), $L_1/H = 5$, $K_1 = 250$ terms.

the normal is therefore also influenced by the boundary conditions. In contrast, the elongation of the normal for a symmetric [0/90/0 deg] thin laminate is insensitive to the boundary conditions at the edges (see Table 5). This is because the normal stresses σ_{11} and σ_{22} in the symmetric laminate are nearly antisymmetric with respect to the midsurface. Thus Poisson's effect at locations on the top half of the laminate is equal and opposite to that at corresponding points on the bottom half, thereby canceling each other's contribution to the average elongation. The elongation of the normal for symmetric laminates is primarily due to σ_{33} at the center of the laminate, which is essentially insensitive to the boundary conditions at the edges. Table 6 gives the through-thickness distribution of the displacements and stresses for the square [0/90/0 deg] laminate that is simply supported on two opposite edges and clamped on the other two. As should be clear from the values of quantities on the two sides of an interface, the continuity of displacements and tractions at the interfaces is satisfied to at least three decimal (significant) digits. The computed value of σ_{33} is off by 0.06% of q_0 on the top and the bottom surfaces of the laminate. This error can be further reduced by retaining more terms in the series expansion.

Figures 7 and 8 show the influence of the boundary conditions on the through-thickness distribution of the normalized transverse shear stress at a section close to the edge $x_1 = 0$. Again, the distribution is not parabolic. For a laminate simply supported on the edges $x_2 = 0$, L_2 and traction free on $x_1 = 0$, L_1, the through-thickness distribution of σ_{13} exhibits stress reversal at points close to the top and bottom surfaces. When the edges $x_1 = 0$, L_1 are rigidly clamped, the curvature of the curve in the central lamina is opposite to that in the two surrounding laminae. A similar behavior is exhibited by the through-thickness distribution of σ_{23} when the boundary conditions at edges $x_1 = 0$, L_1 correspond to B_7 in Table 1. The transverse normal stress distribution depicted in Fig. 9 is also sensitive to the boundary conditions at the edges. When the edges $x_1 = 0$, L_1 are clamped, the through-thickness distribution of σ_{33} at $x_1/L_1 = 0.05$ in the laminate is far from the cubic variation predicted by the CLPT.

When all four edges are simply supported, Pagano[14] has shown that the boundary and the interface conditions can be satisfied by $\boldsymbol{u}^{(n)} = \boldsymbol{u}^{(n,3)}$ in the first equation of Eqs. (18), i.e., the coefficients corresponding to $\boldsymbol{u}^{(n,1)}$ and $\boldsymbol{u}^{(n,2)}$ are zero. This shows the absence of boundary layers near the edges of a simply supported orthotropic

Table 7 Displacement and stresses for a rectangular three-ply laminate clamped on all edges: load (a), $L_1/H = 5$, $L_2/L_1 = 0.5$, $K_1 = 25$ terms

Laminate	$\bar{u}_1(H)$	$\bar{u}_2(H)$	$\bar{u}_3(H/2)$	$\bar{\sigma}_{11}(H)$	$\bar{\sigma}_{22}(2H/3)^a$	$\bar{\sigma}_{12}(H)$	$\bar{\sigma}_{23}(H/2)$	$\bar{\sigma}_{31}(H/2)$
[0/90/0 deg]	−0.10	−0.33	0.35	1.49	1.75	−0.07	2.50	0.64
[45/−45/45 deg]	−0.14	−0.22	0.32	1.10	0.64	−1.48	1.62	0.82

[a]Values corresponding to the central layer.

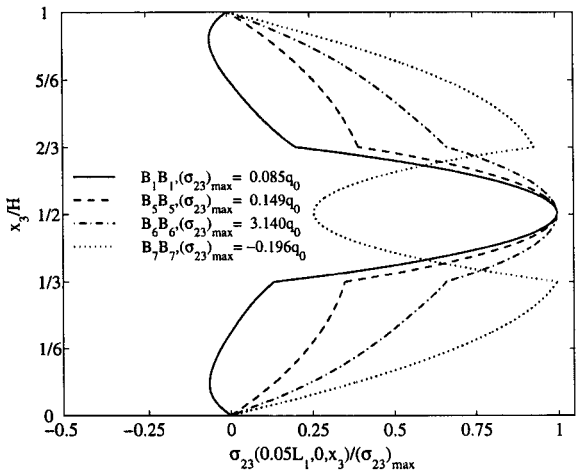

Fig. 8 Influence of the boundary conditions on the through-thickness distribution of the transverse shear stress σ_{23} for a square [0/90/0 deg] laminate: load (a), $L_1/H = 5$, $K_1 = 250$ terms.

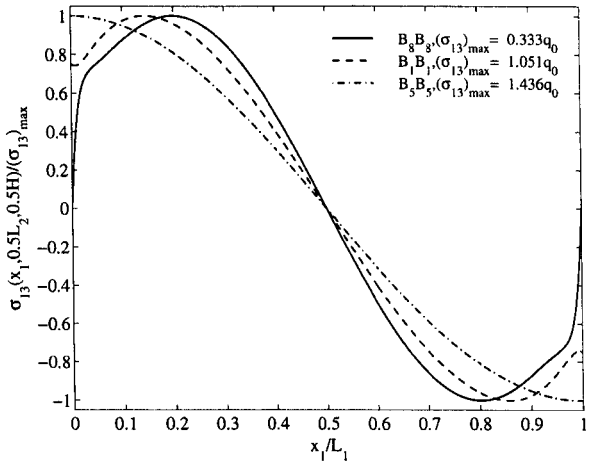

Fig. 10 Variation in the longitudinal direction of the transverse shear stress for a square [0/90/0 deg] laminate for three different boundary conditions: load (a), $L_1/H = 5$, $K_1 = 250$ terms.

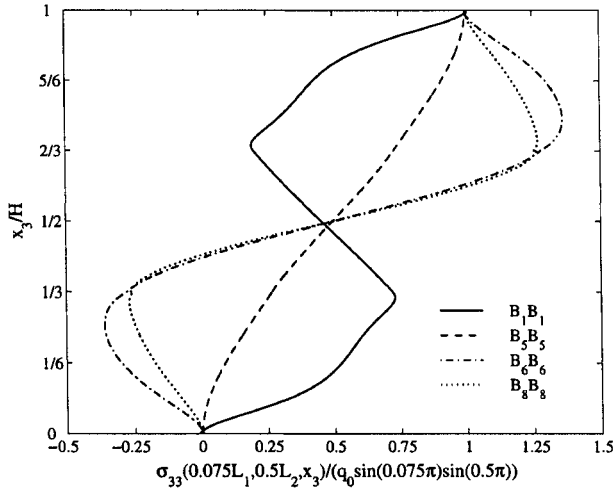

Fig. 9 Influence of the boundary conditions on the through-thickness distribution of the transverse normal stress for a square [0/90/0 deg] laminate: load (a), $L_1/H = 5$, $K_1 = 250$ terms.

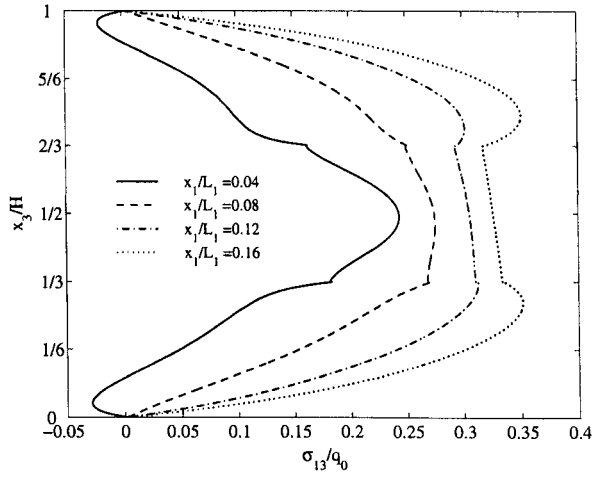

Fig. 11 Through-thickness distribution of the transverse shear stress on four sections of a square [0/90/0 deg] laminate that is simply supported on two opposite edges and traction free on the other two: load (a), $x_2 = L_2/2$, $L_1/H = 5$, $K_1 = 250$ terms.

plate. A boundary layer may exist for boundary conditions other than simply supported edges. Figure 10 shows the transverse shear stress σ_{13} vs x_1 for the square [0/90/0 deg] laminate with two opposite edges simply supported and the other two edges either traction free, clamped, or simply supported. Whereas σ_{13} varies smoothly when the edges $x_1 = 0$, L_1 are simply supported and the curvature of the curve σ_{13} vs x_1 is constant near the edges $x_1 = 0$, L_1, such is not the case when these edges are either clamped or traction free. The thickness of the boundary layer may be equated with the distance from the edge $x_1 = 0$, L_1 of the point where the curvature of the curve σ_{13} vs x_1 suddenly changes. This definition gives the boundary-layer thickness as approximately $0.01L_1$ and $0.03L_1$ near the clamped and the free edges, respectively, for $L_1/H = 5$. The transverse shear-stress distribution close to the free edge for the [0/90/0 deg] laminate that is simply supported on two edges and free on the other two is shown in Fig. 11. It is interesting to note the manner in which the shear stress evolves within the boundary layer adjoining the free edge of the plate into a distribution exhibited by simply supported plates. The preceding definition of the boundary-layer thickness implies that the layer is $0.04H$ near the top and the bottom surfaces of the plate.

B. Clamped Plates

For laminated plates with all four edges clamped, we introduce two additional nondimensional quantities:

$$[\bar{\sigma}_{12}(x_3), \bar{\sigma}_{23}(x_3)] = \left[\frac{10H^2}{q_0 L_1^2}\sigma_{12}\left(\frac{L_1}{8}, \frac{L_2}{8}, x_3\right), \frac{10H}{q_0 L_1}\sigma_{23}\left(\frac{L_1}{2}, \frac{L_2}{8}, x_3\right)\right] \quad (28)$$

Displacements and stresses at specific points in the plate are listed in Table 7 for Cases (2) and (3). Results for $K_1 > 25$ terms have not been computed because of the increased computational effort involved.

VIII. Conclusions

We have generalized the Eshelby–Stroh formalism to study the three-dimensional deformations of linear elastic, anisotropic, laminated rectangular plates subjected to arbitrary boundary conditions at the edges. Equations of elastostatics are satisfied at every point of the body. However, the interface continuity and the boundary conditions are satisfied in the sense of Fourier series. When sufficient terms are included in the analytical series solution, the boundary and the interface continuity conditions are well satisfied at every point on these surfaces.

Our computed results for simply supported plates agree with those of Pagano.[14] For a rectangular laminated plate simply supported on two opposite edges, we have also computed results for nine sets of boundary conditions on the remaining two edges and the plate loaded either on the top or on the bottom surface. One such problem studied involves a square [0/90 deg] laminated plate with two edges of the lower lamina clamped and the corresponding edges of the upper lamina traction free; the other two edges of both laminae are simply supported. Whereas plate theories give same values of the in-plane displacements and in-plane normal stress at points located symmetrically about the midsurface of the plate, we obtain slightly different values of these quantities from the converged solution. The solution, valid for all aspect ratios of the plate, exhibits boundary layers near the clamped and traction-free edges. The transverse shear-stress distributions are found to depend on the boundary conditions as well as on the lamination scheme and are not parabolic. The elongation of the normal to the midsurface of a thick plate depends on whether the transverse load is applied to the top or the bottom surface of the plate and the boundary conditions at the edges. The results presented herein should help establish the validity of various approximate theories.

Note Added in Proof

The authors found two relevant papers (Vlasov, B. F., "On One Case of Bending of Rectangular Thick Plates," *Vestnik Moskovskogo Universiteta. Seriëiìa Matematiki, Mekhaniki, Astronomii, Fiziki, Khimii*, Vol. 2, No. 2, 1957, pp. 25–34; Srinivas, S., and Rao, A. K., "Flexure of Thick Rectangular Plates," *Journal of Applied Mechanics*, Vol. 40, No. 1, 1973, pp. 298, 299) for isotropic thick plates after the submission of the final manuscript. Whereas Vlasov considered simply supported plates, Srinivas and Rao also studied other boundary conditions.

Acknowledgments

This work was partially supported by U.S. Army Research Office Grant DAAG55-98-1-0030 and U.S. National Science Foundation Grant CMS 9713453 to Virginia Polytechnic Institute and State University.

References

[1]Jones, R. M., *Mechanics of Composite Materials*, Scripta, Washington, DC, 1975.

[2]Reddy, J. N., *Mechanics of Laminated Composite Plates: Theory and Analysis*, CRC Press, Boca Raton, FL, 1997.

[3]Whitney, J. M., and Pagano, N. J., "Shear Deformation in Heterogeneous Anisotropic Plates," *Journal of Applied Mechanics*, Vol. 37, No. 4, 1970, pp. 1031–1036.

[4]Lo, K. H., Christensen, R. M., and Wu, E. M., "A High-Order Theory of Plate Deformation, Part 2: Laminated Plates," *Journal of Applied Mechanics*, Vol. 44, No. 4, 1977, pp. 669–676.

[5]Bhimaraddi, A., and Stevens, L. K., "A Higher Order Theory for Free Vibration of Orthotropic, Homogeneous, and Laminated Rectangular Plates," *Journal of Applied Mechanics*, Vol. 51, No. 1, 1984, pp. 195–198.

[6]Reddy, J. N., "A Simple Higher-Order Theory for Laminated Composite Plates," *Journal of Applied Mechanics*, Vol. 51, No. 4, 1984, pp. 745–752.

[7]Di Sciuva, M., "Bending, Vibration and Buckling of Simply Supported Thick Multilayered Orthotropic Plates: An Evaluation of a New Displacement Model," *Journal of Sound and Vibration*, Vol. 105, No. 3, 1986, pp. 425–442.

[8]Murakami, H., "Laminated Composite Plate Theory with Improved In-Plane Responses," *Journal of Applied Mechanics*, Vol. 53, No. 3, 1986, pp. 661–666.

[9]Ren, J. G., "A New Theory of Laminated Plate," *Composites Science and Technology*, Vol. 26, No. 2, 1986, pp. 225–239.

[10]Lee, K. H., Senthilnathan, N. R., and Chow, S. T., "An Improved Zig-Zag Model for the Bending of Laminated Composite Plates," *Composite Structures*, Vol. 15, No. 2, 1990, pp. 137–148.

[11]Noor, A. K., and Burton, W. S., "Assessment of Shear Deformation Theories for Multilayered Composite Plates," *Applied Mechanics Reviews*, Vol. 42, No. 1, 1989, pp. 1–13.

[12]Kapania, R. K., and Raciti, S., "Recent Advances in Analysis of Laminated Beams and Plates, Part 1: Shear Effects and Buckling," *AIAA Journal*, Vol. 27, No. 7, 1989, pp. 923–934.

[13]Pagano, N. J., "Exact Solutions for Composite Laminates in Cylindrical Bending," *Journal of Composite Materials*, Vol. 3, No. 3, 1969, pp. 398–411.

[14]Pagano, N. J., "Exact Solutions for Rectangular Bidirectional Composites and Sandwich Plates," *Journal of Composite Materials*, Vol. 4, No. 1, 1970, pp. 20–34.

[15]Pagano, N. J., and Hatfield, S. J., "Elastic Behavior of Multilayered Bidirectional Composites," *AIAA Journal*, Vol. 10, No. 7, 1972, pp. 931–933.

[16]Srinivas, S., Joga Rao, C. V., and Rao, A. K., "An Exact Analysis for Vibration of Simply-Supported Homogeneous and Laminated Thick Rectangular Plates," *Journal of Sound and Vibration*, Vol. 12, No. 2, 1970, pp. 187–199.

[17]Srinivas, S., and Rao, A. K., "Bending, Vibration and Buckling of Simply Supported Thick Orthotropic Rectangular Plates and Laminates," *International Journal of Solids and Structures*, Vol. 6, No. 10, 1970, pp. 1463–1481.

[18]Rohwer, K., "Application of Higher Order Theories to the Bending Analysis of Layered Composite Plates," *International Journal of Solids and Structures*, Vol. 29, No. 1, 1992, pp. 105–119.

[19]Lee, K. H., and Cao, L., "A Predictor-Corrector Zig-Zag Model for the Bending of Laminated Composite Plates," *International Journal of Solids and Structures*, Vol. 33, No. 6, 1996, pp. 879–897.

[20]Mau, S. T., Tong, P., and Pian, T. H. H., "Finite Element Solutions for Laminated Plates," *Journal of Composite Materials*, Vol. 6, No. 2, 1972, pp. 304–311.

[21]Spilker, R. L., "Hybrid-Stress Eight-Node Elements for Thin and Thick Multilayer Laminated Plates," *International Journal for Numerical Methods in Engineering*, Vol. 18, No. 6, 1982, pp. 801–828.

[22]Liou, W. J., and Sun, C. T., "A Three-Dimensional Hybrid Stress Isoparametric Element for the Analysis of Laminated Composite Plates," *Computers and Structures*, Vol. 25, No. 2, 1987, pp. 241–249.

[23]Ting, T. C. T., *Anisotropic Elasticity. Theory and Applications*, No. 45, Oxford Engineering Science Series, Oxford Univ. Press, New York, 1996.

[24]Eshelby, J. D., Read, W. T., and Shockley, W., "Anisotropic Elasticity with Applications to Dislocation Theory," *Acta Metallurgica*, Vol. 1, No. 2, 1953, pp. 251–259.

[25]Stroh, A. N., "Dislocations and Cracks in Anisotropic Elasticity," *Philosophical Magazine*, Vol. 3, No. 4, 1958, pp. 625–646.

[26]Ting, T. C. T., "Effects of Change of Reference Coordinates on the Stress Analyses of Anisotropic Elastic Materials," *International Journal of Solids and Structures*, Vol. 18, No. 2, 1982, pp. 139–152.

[27]Dempsey, J. P., and Sinclair, G. B., "On the Stress Singularities in the Plane Elasticity of the Composite Wedge," *Journal of Elasticity*, Vol. 9, No. 4, 1979, pp. 373–391.

[28]Huang, K. H., and Dasgupta, A., "A Layer-Wise Analysis for Free Vibration of Thick Composite Cylindrical Shells," *Journal of Sound and Vibration*, Vol. 186, No. 2, 1995, pp. 207–222.

[29]Khdeir, A. A., and Reddy, J. N., "Analytical Solutions of Refined Plate Theories of Cross-Ply Composite Laminates," *Journal of Pressure Vessel Technology*, Vol. 113, No. 4, 1991, pp. 570–578.

S. Saigal
Associate Editor